Electrical conduction in poly(phenylenevinylene) thin films

Electrical conduction in poly(phenylenevinylene) thin films

T P Nguyen†, V H Tran‡ and V Massardier‡

† Laboratoire de Physique Cristalline, Institut des Matériaux de Nantes, 2 rue de la Houssinière, 44072 Nantes Cédex 03, France
‡ Laboratoire des Matériaux Organiques, BP 24, 69390 Vernaison Cédex, France

Abstract. The conduction mechanisms of undoped poly(phenylenevinylene) (PPV) thin films are studied by measuring the current–voltage–temperature characteristics and the thermally stimulated currents in metal–PPV–metal sandwich devices. In the high-temperature range, Poole-Frenkel emission is observed with a mean energy level of the localized states of 0.36 eV from the conduction band. Hopping conduction occurs at lower temperatures with probable interactions between the localized states. Thermally stimulated currents show a complex interface region at the polymer–metal top electrode, confirming previous XPS analysis performed on these devices.

1. Introduction

Of the conjugated polymers, poly(phenylenevinylene) (PPV) is a very promising material for future industrial applications. Because of its very stable nature, this polymer can be easily synthesized and processed to provide thin films with controlled thickness and shape. It is also not sensitive to oxidation and hence can be used as a component in electronic devices. Also, PPV can be doped with current dopants to give a fairly high conductivity (10 S cm^{-1} with AsF$_5$ [1] for example) and remains stable for weeks in an air atmosphere. Recently, the optical properties of this polymer have been studied [2, 3] and very interesting results have suggested the possibility of its application in the fields of non-linear optics and light-emitting diodes. Nevertheless, undoped PPV has been studied less and its electrical properties are relatively unknown, especially the role of the polymer–electrode contacts which are particularly important in electronic devices [4].

We present in this study the results of electrical measurements performed on PPV thin films sandwiched between two metallic layers to form metal–PPV–metal devices. Current–voltage characteristics were studied as a function of the temperature and the nature of the metallic electrodes. Thermally stimulated current (TSC) measurements were also performed to obtain information on the electronic bands of the polymer.

2. Experimental details

PPV thin films were synthesized from a polymer precursor prepared by the method invented by Wessling and Zimmermann [5]. Precursor solutions were cast on well cleaned glass substrates on which bottom electrodes had been previously deposited. After drying under an argon atmosphere, the sample was annealed under a high vacuum in a furnace at 200 °C for several hours to form polymer films. Characterization of the films obtained by absorption measurements showed that the precursor was fully converted [6]. The top electrodes were

then deposited by thermal evaporation of metal at room temperature under high-vacuum conditions (about 10^{-6} Torr). Four samples of 2 mm × 2 mm active area each were obtained on the same substrate. The bottom electrodes were always chromium and the top electrodes used in this work were chromium and aluminium. The thickness of the polymer films, measured with an Alphastep unit, varied from 0.4 to 1.5 μm. The current–voltage characteristics were measured using a Keithley 617 electrometer coupled to a computer to collect the data. The temperature was controlled with a thermocouple scanned by a Keithley 740 system. All measurements were performed under vacuum.

3. Results and discussion

3.1. Current–voltage characteristics

Figure 1 is the plot of the current density versus the applied field, at ambient temperature, for two samples: Cr–PPV–Cr and Cr–PPV–Al. The forward currents are obtained with negative bias of the top electrodes (i.e. Cr or Al). We can see that both of them exhibit rectifying behaviour with a blocking contact on the bottom side (i.e. Cr). The rectifying ratio (forward current density divided by reverse current density) of the Cr–PPV contact is greater than that of Al–PPV. From the polarities of the biased structures, we suggest that electrons are transferred from the top electrodes to the polymer which is p type. The asymmetry of the $I–V$ characteristics may appear surprising at first sight, especially in the case of the Cr–PPV–Cr structure. However, it should be noted that the contacts (PPV–metal and metal–PPV) are formed by different processes and, consequently, their natures may be different. On the other hand, it is known that metals such as aluminium or chromium are very reactive with carbon and oxygen in some polymers [7]. A recent investigation by x-ray photoemission spectroscopy (XPS) [8] of the early stages of the PPV–Al interface formed *in situ* has also shown that a chemical reaction occurs between the polymer and the metal layer to form compounds. Our XPS experiment performed on the interfacial layers has demonstrated that the natures of the top and the bottom interfaces are quite different [9] even for symmetrical structures (Cr–PPV–Cr). At the upper contacts, metallic oxide–carbon complexes are formed and are responsible for the rectifying behaviour as already observed in some amorphous semiconductors [10] or polymers [11]. The rectifying ratio seems to depend directly on the nature of these compounds [9]. On the contrary, at the bottom interface, chromium tends to form clusters embedded in the polymer matrix. This particular behaviour might be explained by a side reaction between the metallic electrode and the products generated during the conversion of the precursor into PPV [9].

Figure 2 is a plot of the direct current versus the inverse of the temperature for several biases in a Cr–PPV–Cr structure. As one can see, these characteristics can be divided into two different parts. In the high-temperature range (say about 200 K), a rapid increase in the current with increasing temperature suggests that the conduction is thermally activated while, in the lower-temperature range, it varies slowly with decreasing temperature. Here, hopping conduction is possible.

In figure 3, the logarithm of the current at different temperatures is plotted against the square root of the applied voltage for these two samples. The straight-line behaviour of the curves can be explained by the Poole–Frenkel mechanism or by Schottky emission at the electrodes [12]. The Schottky emission invokes carriers from the metal electrode into the conduction band over an interfacial barrier which is lowered by the electric field. The current–voltage relationship is given by

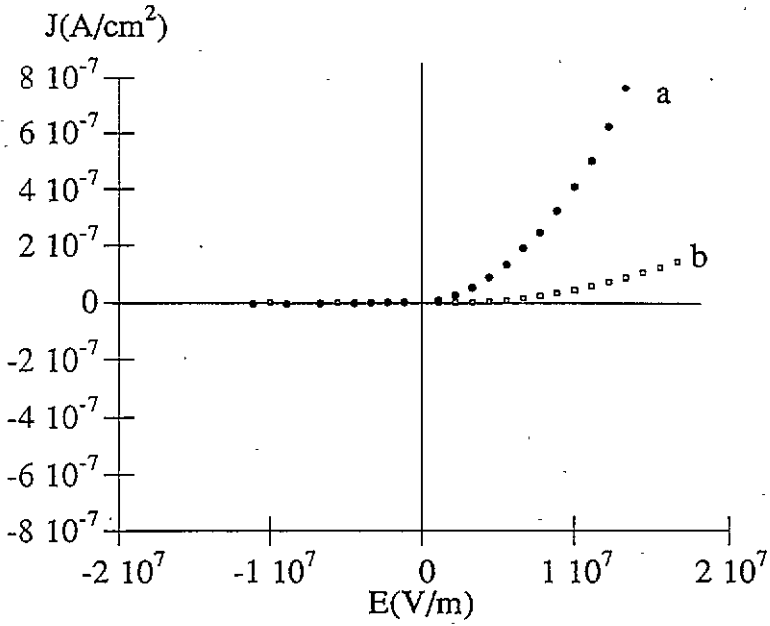$$I = A_0 T^2 \exp\{[\beta_s (V/d)^{1/2} - \phi_s]/kT\} \tag{1}$$

Figure 1. Current density versus applied electric field at $T = 293$ K for a Cr–PPV–Cr structure (curve a) and a Cr–PPV–Al structure (curve b).
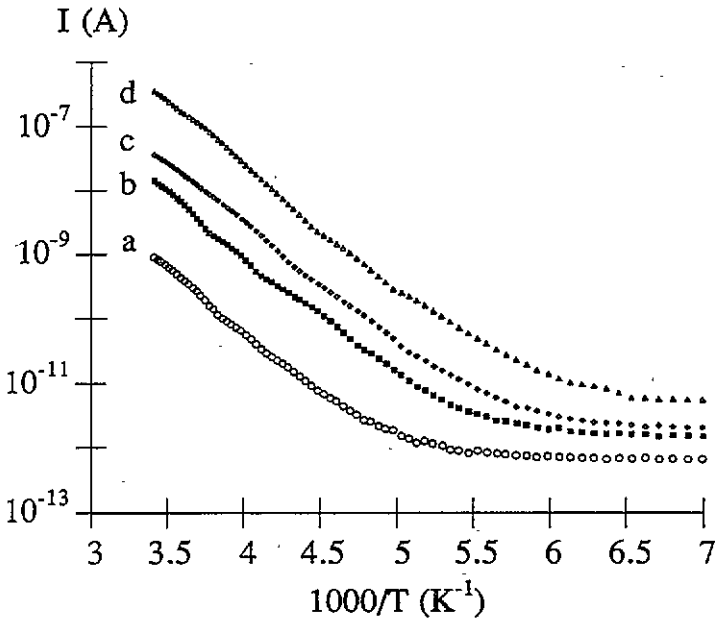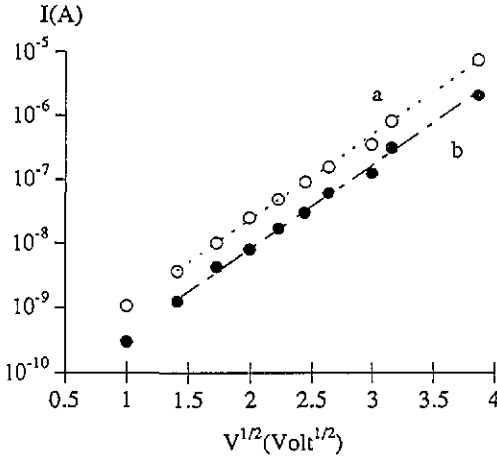

Figure 2. Variation in the logarithm of the current with the inverse temperature for a Cr–PPV–Al structure at different bias voltages: curve a, $V = 1$ V; curve b, $V = 3$ V; curve c, $V = 6$ V; curve d, $V = 9$ V. The thickness of the film is 0.35 μm.

where $\beta_s = (e^3/4\pi\epsilon\epsilon_0)^{1/2}$, A_0 is a constant, e is the electronic charge, d is the thickness of

Figure 3. Plot of the logarithm of the current versus the square root of the applied voltage for a Cr–PPV–Cr structure at different temperatures: line a, $T = 293$ K; line b, $T = 273$ K. The thickness of the film is 0.35 μm.
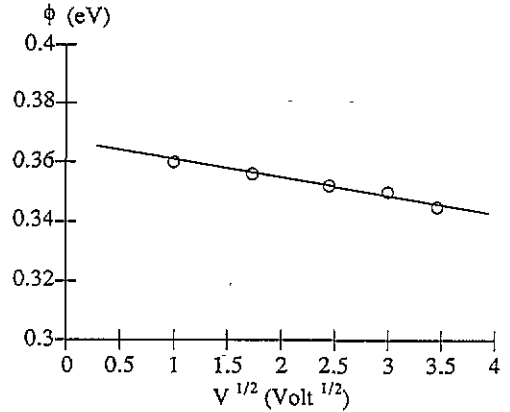
Figure 4. Variation in the activation energy with the square root of the applied field for a Cr–PPV–Cr structure.

the film, ϵ is the relative dielectric constant, ϵ_0 is the dielectric constant of free space and k is the Boltzmann constant. By the Poole–Frenkel mechanism, the conduction is limited by the emission of carriers from localized levels in the bulk into the conduction band as follows:

$$I = B_0 \exp\{[\beta_{PF}(V/d)^{1/2} - \phi_{PF}]/kT\} \tag{2}$$

where $\beta_{PF} = 2(e^3/4\pi\epsilon\epsilon_0)^{1/2} = 2\beta_s$.

To distinguish between these mechanisms, one can evaluate the slope of the curve ln $I = f(V^{1/2})$ and then compare it with theoretical values of the coefficient β. Taking the high-frequency value of the dielectric constant (measured at 500 kHz) of PPV as $\epsilon = 3.2$, we find that the experimental value of $\beta = 9 \times 10^{-25}$ J V$^{1/2}$ m$^{1/2}$ is less than the theoretical values of β_s (= 3.4×10^{-24} J V$^{1/2}$ m$^{1/2}$) and β_{PF} (= 6.8×10^{-24} J V$^{1/2}$ m$^{1/2}$). This result implies that the effective field inside the polymer is higher than the applied field. Similar observations have been made on poly(vinyl chloride) films [13], and in this case no definitive conclusion about the conduction mechanism has been drawn. However, it should be noted that the agreement between the theoretical and experimental values of the coefficient β is not proof of the conduction mechanism since, in many instances, it was found that there was inconsistency between the value of β and the effective conduction in semiconductors (e.g. the experimental value of β can be comparable with β_s although the conduction mechanism is controlled by the Poole–Frenkel effect [14]). In our structures, the modification of the electric field observed might come from the formation of interfacial layers which would reduce the effective thickness of the insulator and therefore introduce a non-uniform electric field through the sample. In this case, it is difficult to verify whether the conduction mechanism is a bulk or a contact process. The activation energy evaluated from the plot of the logarithm of the current versus $1000/T$ is plotted as a function of $V^{1/2}$ and gives a straight line (figure 4). This curve intercepts the ϕ axis at $\phi_0 \sim 0.36$ eV which determines the mean energy level of localized states in the band gap of PPV (in the case of the Poole–Frenkel effect) or the potential barrier height (in the case of the Schottky emission). At this stage, no definitive conclusion can be made without further experimental evidence, as we shall see later.

Next, we investigate the conduction mechanism in the low-temperature range. The activation energy calculated from the experimental curves for all biases yields a very small value (less than 0.05 eV) and suggests that a hopping mechanism probably occurs. A plot of the conductivity σ versus T^{-n} ($n = \frac{1}{4}, \frac{1}{3}$ or $\frac{1}{2}$) is usually performed to identify the hopping process but it should be stressed that, in many cases, this plot gives a straight line with the same data, for any value of the exponent n. Therefore, only physical parameters evaluated from the conduction mechanisms would allow us to distinguish between them. In figure 5, we show the plots $\sigma = f(T^{-n})$ in low-temperature range for different values of the exponent. For clarity, the curves are shifted along the direction of the σ axis and the graduations are not shown. The lowest value of the conductivity is about 10^{-13} S cm^{-1}. Within experimental error, all the curves are linear in the temperature range explored. First, we examine the case where $n = \frac{1}{4}$ which is known as the variable-range-hopping mechanism [15]. This process invokes hops of carriers between localized centres separated by a weak energy difference so that they are more likely than those between nearest centres with greater energy difference. The Mott law for the conductivity gives in this case [16]

$$\sigma = AT^{-1/2} \exp[-(T_{1/4}/T)^{1/4}] \tag{3}$$

where $A = e^2 v[N(E)/32\pi k\alpha]^{1/2}$ and

$$T_{1/4} = \beta_{1/4}^4 \alpha^3 / kN(E). \tag{4}$$

Here $v \, (= 10^{12}\text{--}10^{13} \text{ s}^{-1})$ is the phonon frequency, $N(E)$ is the density of localized states, α^{-1} represents the spatial extent of the defects between which the carriers hop, k is the Boltzmann constant, e is the electronic charge and $\beta_{1/4} \, (= 2.06)$ is a constant.
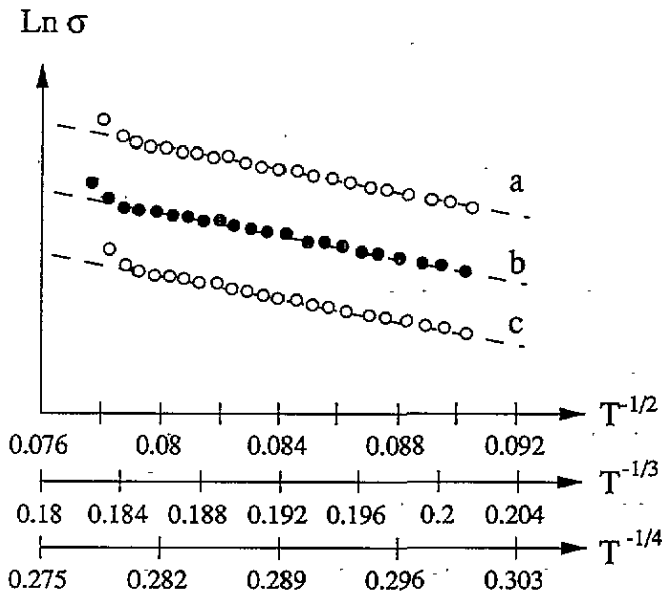
Ln σ

Figure 5. Plot of the conductivity versus T^{-n} for a Cr–PPV–Cr structure: curve a, $n = \frac{1}{2}$; curve b, $n = \frac{1}{3}$; curve c, $n = \frac{1}{4}$. The curves are shifted along the direction of the σ axis for clarity.

The values of the hopping parameters α and $N(E)$ can be evaluated by plotting $\ln(\sigma T^{1/2})$ versus $T^{-1/4}$. The slope of the curve and its intersection with the vertical axis yield $T_{1/4}$ and A, respectively, and from these values we determine α and $N(E)$. It is found that the hopping distance is unreasonably large, which indicates that the Mott model should not be applied in the case of undoped PPV. It must be mentioned that a similar conclusion has been drawn from electrical measurements in undoped [17] or light doped [18] polyparaphenylene (PPP) thin films despite the fact that the $T^{-1/4}$ dependence of $\ln \sigma$ is observed in these cases.

The mechanism with exponent $n \leqslant 3$ is related to two-dimensional hopping and is expected in one-dimensional structures [19]. Considering the thickness of our films (greater than 400 nm), this mechanism might not be effective here.

The $T^{-1/2}$ dependence of the conductivity is found in a hopping mechanism with Coulomb interactions between localized carriers [20]. Owing to these interactions, a soft gap is created in the density states near the Fermi level. The conductivity derived from this hypothesis obeys the Elfros law:

$$\sigma = BT^{-1} \exp[-(T_{1/2}/T)^{1/2}] \tag{5}$$

where B is a constant and $T_{1/2}$ is given by

$$T_{1/2} = \beta_{1/2} e^2 / ka\kappa. \tag{6}$$

$\beta_{1/2}$ is a numerical factor (equal to 2.8), κ is the dielectric constant and a is the hopping distance.

The soft gap can be neglected if the temperature is greater than a critical value T_c given by

$$T_c = (\beta_{1/4}^4 / \beta_{1/2}^2)(T_{1/2}^2 / T_{1/4}). \tag{7}$$

In this case, there will be a transition from the $T^{-1/2}$ dependence to a $T^{-1/4}$ dependence. These considerations allow us to obtain the hopping parameters by plotting $\ln (\sigma T)$ versus $T^{-1/2}$. From the slope of the curve, $T_{1/2}$ can be calculated and a; then the $N(E)$-values are derived from equations (4) and (3). A hopping distance of 50 nm is found with a density of states of about 2×10^{15} eV^{-1} cm^{-3}. These values are comparable with those observed for undoped PPP thin films [17] within the same range of temperatures. This result indicates that PPV thin films have quite compact structures with a low defect density.

3.2. Thermally stimulated current measurements

To complete electrical characterization of PPV thin films, TSC measurements have been carried out on the samples studied before. We recall briefly here the principle of this technique. At a high temperature T_H, the sample is biased at V_b for a sufficiently long time to reach the equilibrium regime. While maintaining the bias, the sample is cooled to a lower temperature T_L and then short circuited. After a new equilibrium regime has been established, the sample is warmed with a constant heating rate R, and the current is monitored simultaneously with the temperature.

Figure 6 shows typical TSC spectra of a Cr–PPV–Cr structure with both polarities (forward and reverse currents) at different biases. The contact effect is clearly shown by the shape of the curves. For reverse current (top electrode positively biased), only one current peak (denoted as peak I) is detected at 180 K while, for the forward direction (top electrode

negatively biased), many other features are observed at higher temperatures in addition to peak I. The intensity of these features increased with increasing bias. However, their shape is not very well defined, indicating that the corresponding localized states are widely distributed in the band gap of the material. From previous results obtained by surface analysis of the PPV–metal interface [9] and from the polarity dependence of the I–V characteristics, we suggest that the additional peaks originate in the interfacial region. We also note that these features are present in all samples (with Cr or Al top electrodes), but that their shapes may differ slightly from one sample to another. The compounds formed at the interface may have a complex structure, and further studies are needed to understand their formation. The results obtained here are similar to those for poly(ethylene tetraphtalate) (PET) [21] for which the TSC spectrum is seen to be strongly affected by the field polarity (structure Au–PET–Al). In this case, the additional peaks are assumed to arise from injection of charge carriers from the electrode (Al). As argued in the (I, V, T) analysis, this hypothesis seems to be verified in the case of our samples. However, it should be stressed that the additional TSC peaks and hence the trapped charges are only observed with a negatively biased top electrode even in the case of a symmetrical structure (Cr–PPV–Cr). This implies that the injected charges in the forward current would be partly trapped by the interfacial layer before reaching the bulk of the film. In the reverse direction, with the applied electric fields used here, in contrast, only the bulk traps would be filled. Consequently, the TSC spectrum presents only one peak, namely peak I. This observation shows the important role of the contact layer in the transport mechanism in polymer thin films. It is known that the metallization of the PET films by Al leads to the formation of an intermixing layer interface [22] and the measured TSC should be related to the formation of this layer.
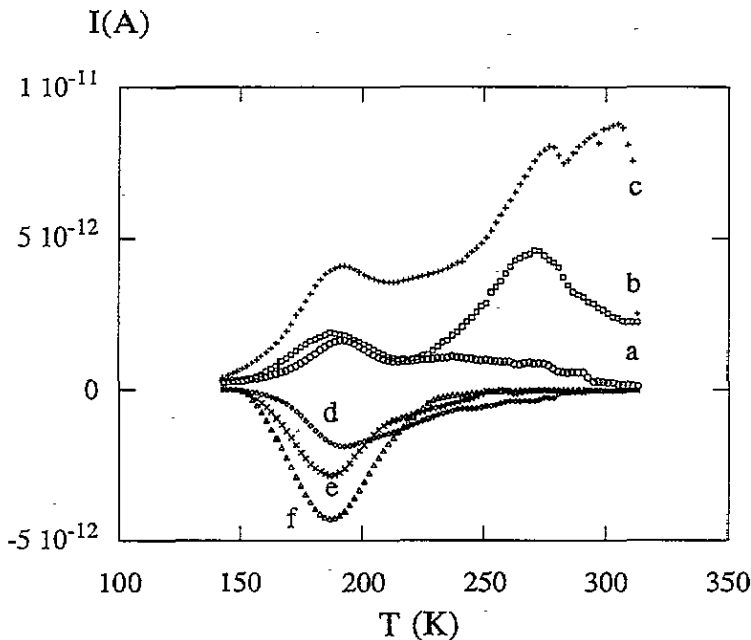
Figure 6. TSC spectra for a Cr–PPV–Cr structure with different bias voltages: curves a and d, $V = 1$ V; curves b and e, $V = 3$ V; curves c and f, $V = 9$ V. The top electrode is negatively biased for curves a–c and positively biased for curves d–f. The thickness of the film is 0.35 μm, $T_H = 293$ K, $T_L = 100$ K and $R = 2.85$ K min^{-1}.

Peak I is reversed when the applied voltage is reversed and we suggest that it originates in the bulk of the films. Its intensity increases but its position is almost unchanged with increasing bias. From the peak temperature, the energy level of trapped charges can be determined using the varying-heating-rate technique. This consists in recording the TSC spectra with the same applied bias and different heating rates. Several analysis methods are available. In the present case, we apply the formulae derived by Booth [23]. Assuming a single relaxation process, the temperature T_M at which the current peak occurs is given by

$$T_M = (\phi/k) R \tau_0 \exp(\phi/kT_M) \qquad (8)$$

where ϕ is the activation energy, R is the heating rate, k is the Boltzmann constant and τ_0^{-1} is the phonon frequency factor. From this relation, the activation energy of the process can be determined by two different heating rates R_1 and R_2 which produce the current peaks at T_{M1} and T_{M2}. A simple calculation furnishes the following expression for ϕ:

$$\phi = [kT_{M1}T_{M2}/(T_{M1} - T_{M2})] \log(R_1 T_{M2}^2 / R_2 T_{M1}^2). \qquad (9)$$

In figure 7, the TSC spectra of Cr–PPV–Cr is recorded with different heating rates at the same applied bias. The current peak is shifted to higher temperatures with increasing R but the relaxed charges (measured by integrating the area under the curves) remain approximately constant. Equation (9) yields a value of $\phi = 0.35 \pm 0.03$ eV which is close to that determined at high temperatures in the $I(V, T)$ characteristics studied above. Therefore, the same localized states would be reponsible for both conduction mechanisms. Furthermore, a fit using the Cowell–Woods [24] formula (broken curve) shows that there would be a distribution of traps centred on the energy level found. The trap depths corresponding to peaks P_2 and P_3 determined by the same technique are 0.68 eV and 0.82 eV, respectively. From this result, we can confirm that the effective conduction mechanism in the high-temperature range is related to the bulk of the films (i.e. the Poole–Frenkel effect) since it involves the same localized states as in the charge relaxation which is obviously a bulk mechanism. Note that the TSC measurements have demonstrated the existence of a very complex interfacial region near the top electrode of the structures which has already been revealed by XPS analysis [9] and which is the origin of the rectifying contacts observed in our structures. These layers act as intermediates between the metal and the polymer so that the classical notion of a Schottky barrier should not have its full meaning here [25]. They also explain why the $I-V$ characteristics seem to be independent of the work function of the electrode metals. Future spectroscopic analyses (IR, Raman, etc) are necessary for a better understanding of the formation conditions of these layers.

4. Conclusion

In summary, we have studied the conduction mechanisms in PPV thin films sandwiched between two metallic electrodes. We have found that the Poole–Frenkel effect occurs in the high-temperature range while hopping conduction with Coulomb interactions between localized electrons is likely in the low-temperature range. The defect density in the films is found to be about 10^{15} cm^{-3}, indicating that they are very compact. TSC measurements have indicated interfacial effects in the PPV–metal contacts and confirmed previous XPS results obtained for these structures. The energy level of localized states in the polymer determined from both $I(V, T)$ and TSC characteristics is located at 0.36 eV from the conduction band.
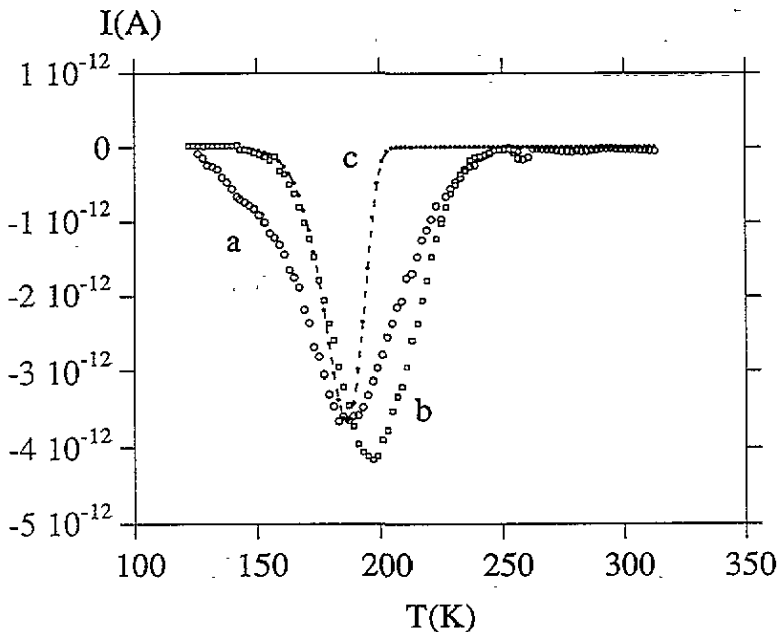
Figure 7. TSC spectra for a Cr–PPV–Cr structure with different heating rates: curve a, $R = 2.85$ K min^{-1}; curve b, $R = 8.7$ K min^{-1}; curve c, the Cowell–Woods fitted curve with $R = 2.85$ K min^{-1}. The thickness of the film is 0.35 μm, $T_H = 293$ K, $T_L = 100$ K and $V = 9$ V. The top electrode is negatively biased for all curves.

References

[1] Karasz F E, Capistran J D, Gagnon D R and Lenz R W 1985 *Mol. Cryst. Liq. Cryst.* **118** 327
[2] Burroughes J H, Bradley D D C, Brown A R, Marks R N, Mackay K, Friend R H, Burns P L and Holmes A B 1990 *Nature* **347** 539
[3] Braun D and Heeger A J 1992 *Thin Solid Films* **216** 96
[4] Forrest S R, Kaplan M L, Schmidt P H, Feldmann W L and Yanowski E 1982 *Appl. Phys. Lett.* **41** 90
[5] Wessling R A and Zimmermann R G 1968 *US Patent* 3,401,152
[6] Wung C J, Pang Y, Prasad P N and Karasz F E 1991 *Polymer* **32** 605
[7] Pireaux J J, Gregoire C, Vermeerch M, Thiry P A and Caudano R 1987 *Surf. Sci.* **189** 903
[8] Lazzaroni R, Fredriksson C, Calderone A, Bredas J L, Dannetun P, Boman M, Stafström S and Salaneck W R 1993 *Synth. Metals* at press
[9] Nguyen T P, Tran V H, Massardier V and Guyot A 1993 *Synth. Met.* **55–57** 235
[10] Fritzsche H 1970 *Electronic and Structural Properties of Amorphous Semiconductors* ed L I Maissel and R Glang (New York: McGraw Hill) p 55
[11] Guillaud G, Boujema B, Gamoudi M, Ranaivo-Harisoa R, Andre J J, François B and Mathis C 1985 *Synth. Met.* **10** 397
[12] Simmons J G 1971 *J. Phys. D: Appl. Phys.* **4** 613
[13] Bahri R and Singh H P 1980 *Thin Solid Films* **69** 281
[14] Jonscher A K and Ansari A 1971 *Phil. Mag.* **23** 205
[15] Mott N F 1968 *J. Non-Cryst. Solids* **1** 1
[16] Nagels P 1979 *Amorphous Semiconductors* ed M H Brodsky (Berlin: Springer) p 113
[17] Nguyen T P, Ettaik H, Lefrant S and Leising G 1991 *Synth. Met.* **44** 45
[18] Stubb H, Isolato H, Kuivalainen P, Raatikainen P and Holmström C 1983 *J. Phys. C: Solid State Phys.* **3** 737
[19] Hamilton E M 1972 *Phil. Mag.* **26** 104
[20] Efros A L and Shlovskii B 1 1985 *Electron–Electron Interaction in Disordered Systems* ed A L Efros and M Pollak (Amsterdam: North-Holland) p 409

[21] Kojima K, Meada A and Ieda M 1976 *Japan. J. Appl. Phys.* **15** 2457
[22] Bou M, Martin J M, Le Mogne T and Vovelle L 1991 *Appl. Surf. Sci.* **47** 149
[23] Booth A H 1954 *Can. J. Chem.* **32** 214
[24] Cowell T A T and Woods J 1967 *Br. J. Appl. Phys.* **18** 1045
[25] Brillson L J 1983 *J. Phys. Chem. Solids* **44** 703